

1 Adsorption of Laminin on Hydroxyapatite and 2 Alumina and the MC3T3-E1 Cell Response

3 *Hiroka Fujita[†], Tada-aki Kudo[‡], Hiroyasu Kanetaka[‡], Toshiki Miyazaki[§], Masami Hashimoto[¶],*
4 *and Masakazu Kawashita^{*,†}*

5 [†] Graduate School of Biomedical Engineering, Tohoku University, Aoba-ku, Sendai 980-8579,
6 Japan

7 [‡] Graduate School of Dentistry, Tohoku University, Aoba-ku, Sendai 980-8575, Japan

8 [§] Graduate School of Life Science and Systems Engineering, Kyushu Institute of Technology,
9 Wakamatsu-ku, Kitakyushu 808-0196, Japan

10 [¶] Japan Fine Ceramics Center, Atsuta-ku, Nagoya 456-8587, Japan

11 ABSTRACT: Artificial hydroxyapatite (HAp) is osteoconductive, but the mechanism is still
12 unclear. It is likely that some serum proteins are adsorbed onto HAp and influence its
13 osteoconductivity. We investigated the adsorption behavior of laminin (LN), which was isolated
14 from murine Engelbreth-Holm-Swarm sarcoma, onto HAp and compared it with non-
15 osteoconductive alpha-type alumina (α -Al₂O₃). Cell adhesion, spreading, and proliferation on
16 native and LN-adsorbed discs of HAp or α -Al₂O₃ were examined using murine MC3T3-E1
17 osteoblastic cells. A larger amount of LN adsorbed onto HAp than α -Al₂O₃ despite the
18 electrostatic repulsion between LN and HAp, suggesting the specific adsorption of LN onto
19 HAp. The LN adsorbed onto HAp remarkably enhanced initial attachment and spreading of

1
2
3 1 MC3T3-E1 cells, but subsequent proliferation of MC3T3-E1 cells was influenced by the type of
4
5 2 material rather than LN adsorption. These fundamental findings imply that LN adsorbed on HAp
6
7 3 could trigger osteoconductivity *in vivo*, aiding in the development of novel biomaterials that
8
9 4 specifically-adsorb LN and effectively enhance cell attachment and spreading.
10
11
12
13

14 5 KEYWORDS: adsorption, laminin, hydroxyapatite, α -alumina, bioactivity, osteoconductivity,
15
16 6 MC3T3-E1
17
18
19
20
21

22 8 1. INTRODUCTION

23
24

25 9 Hydroxyapatite (HAp) is dominant in the inorganic phase of hard tissue, such as bone and
26
27 10 teeth in vertebrates. Since the discovery of the excellent osteoconductivity of artificial HAp that
28
29 11 was experimentally implanted into the body of live mammals in the 1970s^{1,2}, HAp has been
30
31 12 widely used as an osteoconductive (i.e. bioactive) bone substitute^{3,4} or coating material to induce
32
33 13 bioactivity of bio-inert orthopedic and dental implants^{5,6}. However, the detailed mechanism of
34
35 14 the osteoconductivity of HAp is still unclear. Phenomenological reactions at the bone-material
36
37 15 interface, which consist of six stages: (1) serum protein adsorption onto the implanted material,
38
39 16 (2) recruitment of cells such as pluripotent progenitors, (3) attachment and proliferation of the
40
41 17 cells, (4) differentiation and activation of the cells, (5) matrix calcification, and (6) bone
42
43 18 remodeling, have been proposed⁷. Initial protein adsorption may occur on any material implanted
44
45 19 into the body regardless of its osteoconductivity. Therefore, we hypothesize that specific proteins
46
47 20 adsorbed onto HAp may trigger osteoconductivity.
48
49
50
51
52
53

54 21 Based on our hypothesis, we have been focusing on initial protein adsorption and its effect on
55
56 22 cell response. Thus, we have examined albumin and fibronectin as a cell adhesion inhibitory
57
58
59
60

1 protein and cell-adhesive protein, respectively. We previously investigated the adsorption
2 behavior of these proteins^{8,9} and the effect of adsorbed proteins on cellular responses^{10,11}. As a
3 result, we obtained experimental results implying that the quick adherence of osteoblast cells and
4 monocyte-macrophage lineage cells prior to albumin adsorption likely plays a role in the
5 induction of HAp osteoconductivity¹⁰ and that the fibronectin specifically adsorbed on HAp
6 enhances adhesion and spreading of pre-osteoblast cells, which may contribute to HAp
7 osteoconductivity¹¹.

8 In addition to albumin and fibronectin, laminin (LN) is a cell-adhesive protein that plays an
9 important role in HAp osteoconductivity. Numerous serum proteins adsorb simultaneously on
10 artificial HAp *in vivo*, and there is a possibility that the adsorbed proteins control HAp
11 osteoconductivity via a concerted mechanism. However, it is still important to investigate the
12 roles of specific proteins such as laminin in HAp osteoconductivity. LN is a basement membrane
13 protein with a molecular weight of 850 kDa and is contained at a concentration of 0.81–1.43
14 $\mu\text{g/mL}$ in human serum¹². LN has three subunits of α , β , and γ chains, and these chains provide
15 more than ten types of LN isoforms¹³. The subunits of LN assemble at the C-terminate and N-
16 terminate to form long and short arms, respectively, and hence LN is folded into the shape of a
17 cross¹³. Further, LN has a domain that binds to the extracellular matrix and cell via integrins¹⁴,
18 and the α chain of LN promotes odontoblast cell adhesion and differentiation¹⁵. It was confirmed
19 that LN-HAp coating on titanium and ethylene vinyl alcohol copolymer enhanced epithelial-like
20 cell adhesion^{16,17}. More recently, it was found that the specific sequence within human LN
21 causes the enhancement of bone cell functions *in vitro* and induces faster osseointegration *in*
22 *vivo*¹⁸, and adhesion and spreading of osteoblast-like cells seeded on the LN-derived core
23 peptide-coated surface were detected¹⁹. Further, the doubling time of human mesenchymal stem

1 cells or MG-63 human osteoblast-like cells was found to be reduced by LN coating^{20,21},
2 suggesting that laminin might enhance proliferation of osteoblasts. However, to the best of our
3 knowledge, there is no comparative study on LN adsorption on bioactive HAp and bio-inert
4 alpha-type alumina (α -Al₂O₃) and its effect on cell response. α -Al₂O₃ and HAp are traditional
5 ceramic components of orthopedic and dental implants, but they do not exhibit osteoconductivity
6 (bio-inert)^{22,23}. Therefore, α -Al₂O₃ is a representative bio-inert ceramic for investigation of HAp
7 osteoconductivity. In the present study, we investigated adsorption behavior of LN on HAp and
8 α -Al₂O₃ as well as the response of osteoblast-like murine-derived MC3T3-E1 cells directly
9 seeded on these LN-coated materials.

10 2. EXPERIMENTAL (MATERIALS AND METHODS)

11 2.1. Sample preparation

12 Commercially available HAp (ca-HAp) powder (HAP-200, Taihei Chemical Industrial Co.
13 Ltd., Osaka, Japan), α -Al₂O₃ (ca-Al₂O₃) powder (ALO14PB, Kojundo Chemical Lab. Co. Ltd.,
14 Saitama, Japan), and laminin (LN) of the Engelbreth-Holm-Swarm (EHS) murine sarcoma that is
15 a representative rich source of basement membrane components (LN concentration: 1–2 mg/mL,
16 L2020, Sigma Aldrich, St. Louise, MI, USA) were used in the present study. In order to examine
17 the effect of crystal orientation on LN adsorption behavior, HAp powders orientated to the c-axis
18 (a(b)-HAp powder) were prepared via the urea homogenous precipitation method^{24,25} and those
19 oriented to the a(b)-axis (c-HAp powder) were prepared according to Zhuang's method²⁵.

20 2.2. Measurement of specific surface area and zeta potential of samples

1 Adsorption behavior of LN is remarkably affected by the physical and chemical properties of
2 HAp and α -Al₂O₃. We already reported the morphology, crystalline phase, and crystal
3 orientation of ca-HAp, a(b)-HAp, c-HAp, and ca-Al₂O₃ powders⁹. Therefore, in the present study,
4 ca-HAp, a(b)-HAp, c-HAp, and ca-Al₂O₃ powders were heated for 2 h at 200 or 300°C, and the
5 specific surface area (SSA) of these materials was measured using the Brunauer-Emmett-Teller
6 (BET) technique (Autosorb[®]-iQ-MP, Quantachrome Instruments, Boynton Beach, FL, USA).
7 Further, the zeta potentials of ca-HAp, a(b)-HAp, c-HAp, and ca-Al₂O₃ powders and LN in
8 phosphate-buffered saline (PBS; Wako Pure Chemicals, Osaka, Japan) at 35°C were measured
9 using electrophoresis spectroscopy (Zetasizer Nano ZS90, Malvern Instruments Ltd.,
10 Worcestershire, UK). The measurement was conducted twice, and the applied voltage was
11 maintained at 3–5 mV.

12 2.3. Measurement of adsorption capacity of LN on HAp and α -Al₂O₃ powders

13 LN was mixed with PBS for 24 h at 4°C to obtain LN solutions with different concentrations
14 of 0.125–0.9 mg/mL. Tubes containing 2.8 mg ca-HAp powder or 6.67 mg ca-Al₂O₃ powder
15 were incubated with 300 μ L LN solutions with different concentrations, respectively, at 36.5°C
16 for 1 h while rotating at 5 rpm using a tube rotator (TR-350, As One Corp., Osaka, Japan). The
17 mixture was centrifuged for 10 min at 10,000 rpm (H-201F, Kokusan Co., Ltd., Saitama, Japan),
18 and the supernatant was collected by micropipette (Nichipet EXII, Nichiryō Co., Ltd., Saitama,
19 Japan). The supernatant of 100 μ L was put into a 70 μ L-disposable cell (UV-Cuvette micro,
20 BrandTech Scientific Inc., Essex, CT, USA), and the concentration of LN in the supernatant was
21 measured by UV-Vis spectrometer (V-730BIO, Jasco Corp., Tokyo, Japan). For the LN
22 concentration measurement, an ultraviolet absorption method with optical path length of 10 mm

1 was employed, and the LN concentration was estimated by the Warburg-Christian method²⁶. The
2 adsorbed amount of LN was calculated by the LN concentration in the supernatant. A similar
3 measurement was performed for a(b)-HAp and c-HAp powders in 0.5 mg/mL LN solution.
4 Statistical analysis was performed for adsorption capacity of LN on ca-HAp and ca-Al₂O₃
5 powders at each LN concentration using ANOVA, and *P*-values < 0.05 were considered
6 significant.

7 2.4. Measurement of secondary structure of LN adsorbed on samples

8 The secondary structure of LN adsorbed on the samples was measured by Fourier transform
9 infrared (FT-IR) spectroscopy as follows. Samples soaked in LN solutions were freeze-dried
10 (FD-1000, Tokyo Rikakikai, Tokyo, Japan). A moderate amount of the freeze-dried samples was
11 placed on a potassium bromide (KBr) plate (2000-0060, Jasco Corp., Tokyo, Japan) and pressed
12 against another KBr plate at a pressure of 10 kN to form a KBr pellet 5 mm in diameter. The
13 KBr pellet was subjected to FT-IR measurement at a resolution of 4 cm⁻¹ and a cumulated
14 number of 16.

15 2.5. MC3T3-E1 cell adhesion, spreading, and proliferation assay

16 Commercially available HA powder (HAP-200; Taihei Chemical Industrial Co., Osaka, Japan)
17 was molded in a metal die and then cold isostatically pressed (CIP; MODEL 30X; Kobe Steel,
18 Hyogo, Japan) at 245 MPa to form 14 mm diameter discs. The discs were sintered at 1300°C for
19 1 h in air. A temperature of 30°C/min was used for heating and furnace cooling was used to cool
20 the samples. For the present study, 14-mm diameter α-Al₂O₃ discs were purchased from a
21 commercial supplier (SSA-S; Heat System Co., Fukuoka, Japan). The discs were then polished
22 with a 400 grit-diamond polishing sheet (Maruto Instrument Co., Ltd, Tokyo, Japan) to produce

1 a uniform surface roughness. Prior to experimentation, discs were washed with acetone, ethanol,
2 and distilled water. These discs were named “untreated discs” in the present study. It was already
3 confirmed in our previous study that no other unexpected crystalline phase was contained in
4 these samples by examining the thin film X-ray diffraction patterns for peaks other than those of
5 HAp and α -Al₂O₃ and that any difference in surface morphology and roughness between HAp
6 and α -Al₂O₃ discs that might affect protein adsorption and cell response was considerably
7 reduced¹⁰.

8 Untreated HAp and α -Al₂O₃ discs were autoclaved at 121°C for 20 min. The disc samples
9 were placed on a 24-well low-attachment plate (Corning 3473, Corning Inc., Corning, NY, USA),
10 and 0.5 mL of LN solution at 0.4 or 0.8 mg/mL was poured into each well. Then, the plate was
11 kept at 4°C for 1 h, and the supernatant of LN solution was removed from each well by
12 micropipette to provide LN-adsorbed disc samples. Table 1 summarizes the names of the
13 samples used in the present study. MC3T3-E1 osteoblast-like cells were seeded at 10,000 cells
14 per well onto each disc placed onto the bottom of each well that was filled with 1 mL of
15 Dulbecco’s Modified Eagle’s medium supplemented with 20% fetal bovine serum and
16 penicillin/streptomycin. To more accurately evaluate the behaviors of the cultured cells on the
17 sample materials, the employed discs were placed onto the bottom of each well of a non-culture
18 plate (351147, Techno Plastic Products AG, Trasadingen, Switzerland), to reduce any
19 proliferation of the incubated cells in the narrow area around the disc in each well. For
20 experiments, the cells were cultured for various periods of time ranging from 1 h to 7 days at
21 37°C and 5% CO₂.

1
2
3 1 For cell adhesion and spreading assays, live MC3T3-E1 cells adhered to sample discs were
4
5 2 stained with a cell permeant viability probe fluorescein diacetate (FDA; Dojindo Laboratories,
6
7
8 3 Kumamoto, Japan), the number of adhered cells was counted, and the maximum cell length was
9
10 4 measured using an inverted fluorescent microscope (CKX41, Olympus, Tokyo, Japan) equipped
11
12 5 with a digital camera (DP72, Olympus, Tokyo, Japan) and laser light source (U-RFLT50,
13
14 6 Olympus, Tokyo, Japan). To evaluate cell proliferation by measuring the amount of total DNA
15
16 7 harvested from cells on sample materials, we isolated DNA from the adhered cells in a 24-well
17
18 8 non-culture plate (351147, Techno Plastic Products AG, Trasadingen, Switzerland) at 1, 3, and 7
19
20 9 days after incubation using the AllPrep DNA/RNA/Protein Mini Kit and QIA Shredder columns
21
22 10 (Qiagen, Hilden, Germany), according to the manufacturer's protocol. To ensure the complete
23
24 11 cell extraction from the discs, cell scrapers (Sumitomo Bakelite Co., Tokyo, Japan) were used in
25
26 12 combination with lysis buffer (RLT buffer) included in the DNA extraction kit, and DNA was
27
28 13 quantified by measuring the absorbance at 260 nm using a spectrophotometer (e-spect, BM
29
30 14 Equipment Co., Ltd., Tokyo, Japan). Statistical analysis was performed using ANOVA and
31
32 15 Tukey's test, and *P*-values < 0.05 were considered significant.
33
34
35
36
37
38
39
40 16
41
42
43 17 **Table 1.** Disc samples used for the cell culture test.
44
45
46
47
48
49
50
51
52
53
54
55
56
57
58
59
60

Sample name	Material	Concentration of LN solution [mg/mL]
LN0-HA	Hydroxyapatite	0 (untreated)
LN4-HA	Hydroxyapatite	0.4
LN8-HA	Hydroxyapatite	0.8
LN0-AL	α -Al ₂ O ₃	0 (untreated)
LN4-AL	α -Al ₂ O ₃	0.4
LN8-AL	α -Al ₂ O ₃	0.8

3. RESULTS

3.1. Adsorption behavior of LN on HAp and α -Al₂O₃ powders

Table 2 shows SSAs and zeta potentials of HAp and α -Al₂O₃ powders and LN in PBS. The ca-HAp, a(b)-HAp, and c-HAp powders and LN were negatively charged whereas ca-Al₂O₃ powder was positively charged in PBS. Based on the SSAs, the surface area of HAp and α -Al₂O₃ powders used to investigate the adsorption behavior of LN was adjusted to 0.04 m².

Table 2. SSAs and zeta potentials of samples.

Sample	SSA [m ² /g]	Zeta potential [mV]
ca-HAp	8.69	-12.8
ca-Al ₂ O ₃	3.65	3.4
(a)b-HAp	5.17	-7.9
c-HAp	17.37	-28.6
LN	—	-6.9

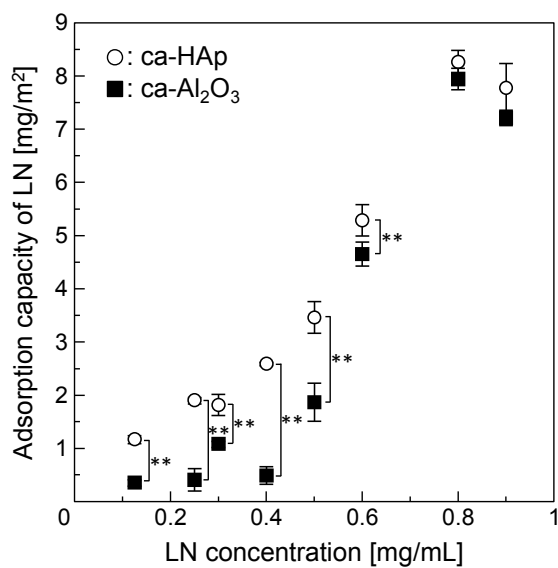
Figure 1 shows isotherms for the adsorption of LN onto ca-HAp and ca-Al₂O₃ powder. The adsorption amount of LN gradually increased in a concentration-dependent manner irrespective of the type of powder, and the capacity of ca-HAp powder (1.17–5.29 mg/m²) was remarkably higher than ca-Al₂O₃ powder (0.35–4.65 mg/m²) at 0.125–0.6 mg/mL LN solution

1 concentrations. However, the adsorption capacity of LN was almost saturated at concentrations
 2 over 0.8 mg/mL in both materials examined, and there was no significant difference in the LN
 3 adsorption capacity between HAp and ca-Al₂O₃ powder.

4 The Langmuir equation is often used to analyze isotherms, but sometimes it is inadequate for
 5 protein adsorption²⁷. When interaction between proteins is not negligible, the following Hill
 6 equation is often used²⁷⁻²⁹:

$$q = \frac{K_h C^n q_0}{1 + K_h C^n} \quad (1)$$

7 where q is the amount of adsorption, q_0 is the saturated amount of adsorption, K_h is the
 8 equilibrium constant in the Hill model, C is the equilibrium concentration, and n is the Hill
 9 coefficient. The determination coefficients (R^2) for the LN adsorption isotherm on ca-HAp
 10 powder and ca-Al₂O₃ powder calculated using the Hill equation were 0.914 and 0.933,
 11 respectively. The Hill coefficients (n) were 1.322 for ca-HAp powder and 2.611 for ca-Al₂O₃
 12 powder.
 13 powder.



14

1 **Figure 1.** Isotherms for adsorption of LN onto ca-HAp and ca-Al₂O₃ powders (mean ± SD, ***P*

2 < 0.01).

3 Figure 2 shows the LN adsorption capacity of ca-HAp, a(b)-HAp, and c-HAp powders in 0.5

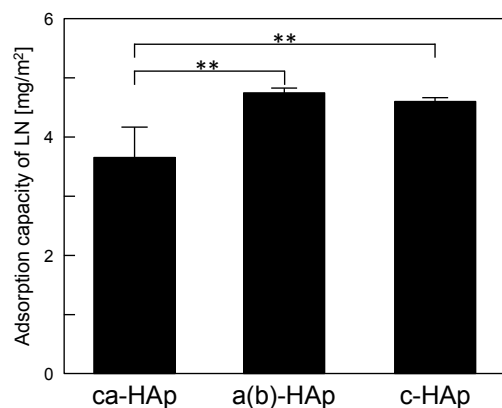
4 mg/mL LN solution. The LN adsorption capacities of a(b)-HAp and c-HAp powder were

5 significantly higher than ca-HAp powder. Table 3 shows the secondary structure of LN adsorbed

6 on ca-HAp, a(b)-HAp, c-HAp, and ca-Al₂O₃ powders in 0.5 mg/mL LN solution. No significant

7 difference was observed in the secondary structure of adsorbed LN between samples (α -helix:

8 13–14%, β -sheet: 33–35%, β -turn: 24–29%, others: 22–29%).



9 **Figure 2.** LN adsorption capacity of ca-HAp, a(b)-HAp, and c-HAp powders in 0.5 mg/mL LN

10 solution (mean ± SD, ***P* < 0.01).

11 **Table 3.** Secondary structure of LN adsorbed on ca-HAp, ca-Al₂O₃, a(b)-HAp, and c-HAp

12 powders in 0.5 mg/mL LN solution.

13

Sample	α -helix [%]	β -sheet [%]	β -turn [%]	Others [%]
ca-HAp	14	34	25	27
ca-Al ₂ O ₃	13	34	24	29
a(b)-HAp	14	33	25	28
c-HAp	14	35	29	22

3.2. MC3T3-E1 cell response to samples

Figure 3 shows the number of MC3T3-E1 cells that adhered onto HAp and α -Al₂O₃ discs. The number of MC3T3-E1 cells that adhered onto HAp was relatively higher than α -Al₂O₃ regardless of LN adsorption, and it remarkably increased on samples LN8-HA and LN8-AL after a culture period of 6 h. However, there was no significant difference between the number of MC3T3-E1 cells adhered onto sample LN0-HA and sample LN0-AL at each culture period.

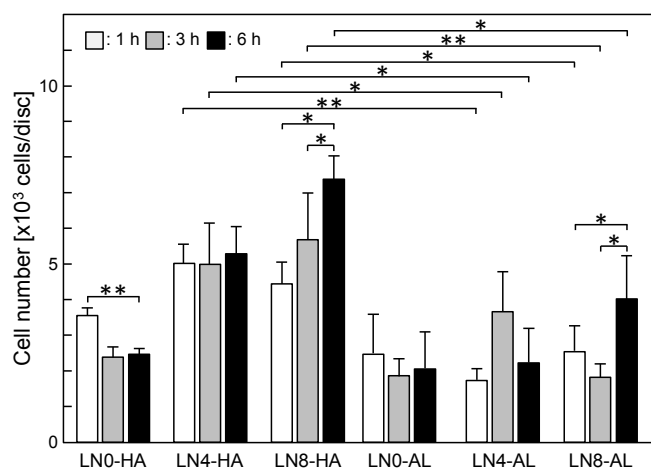
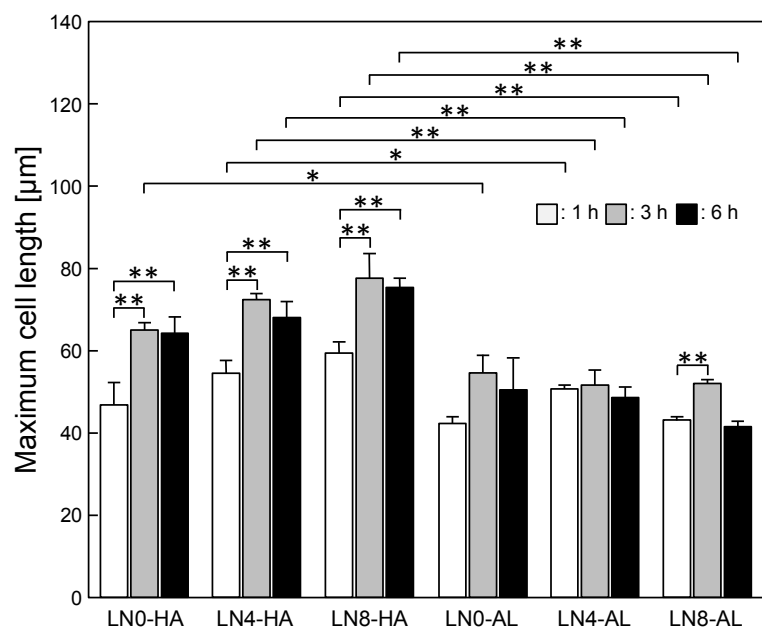


Figure 3. Number of MC3T3-E1 cells adhered to HAp and α -Al₂O₃ discs (mean \pm SD, * P < 0.05, ** P < 0.01).

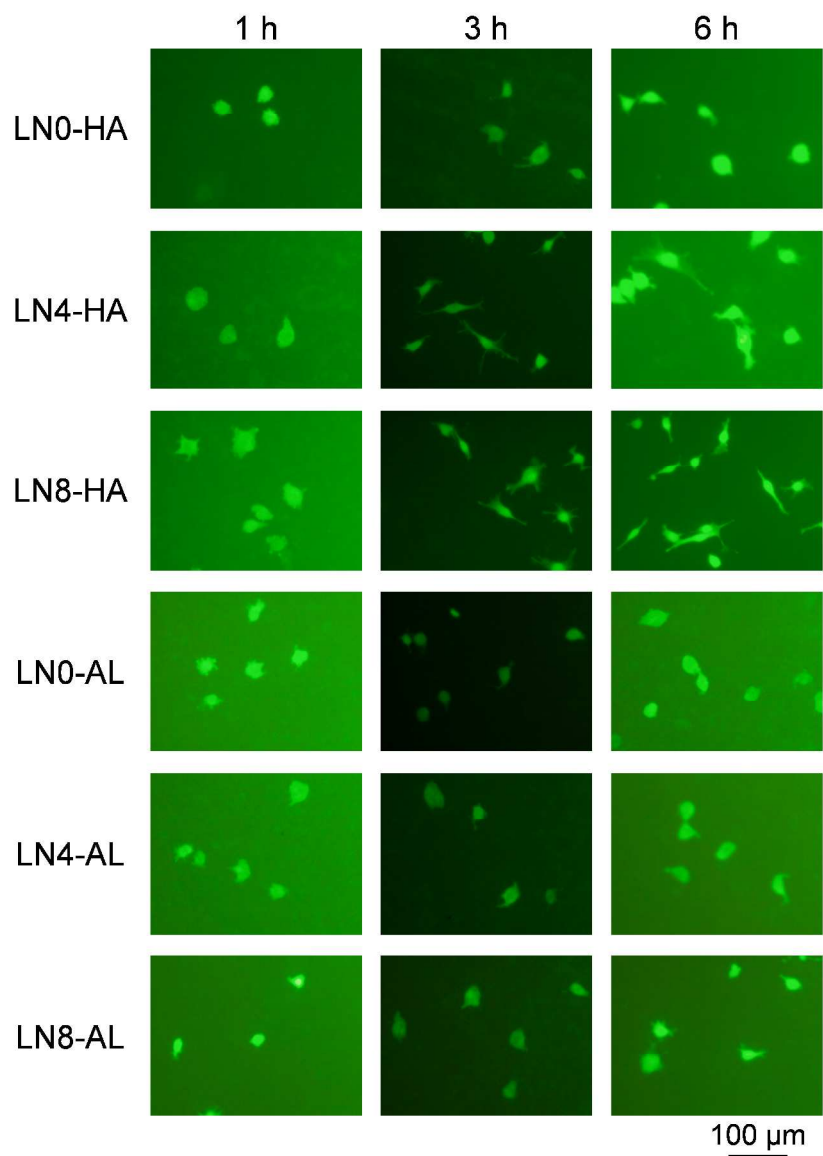
Figure 4 shows the maximum length of MC3T3-E1 cells adhered onto HAp and α -Al₂O₃ discs. The adhered MC3T3-E1 cells spread considerably on HAp discs after culture periods of 3 and 6 h, but the cells hardly spread on α -Al₂O₃ discs even after 6 h irrespective of LN adsorption.

1 However, there was no significant difference in the cell spreading between samples LN0-HA and
 2 LN0-AL. Figure 5 shows representative fluorescent microscopic images of MC3T3-E1 cells
 3 adhered to HAp and α -Al₂O₃ discs. After a culture period of 6 h, cell spreading was observed on
 4 LN-adsorbed HAp discs (samples LN4-HA and LN8-HA) but not on α -Al₂O₃ discs (samples
 5 LN0-AL, LN4-AL, and LN8-AL). Figure 6 shows the time-dependent variation in the DNA
 6 concentration harvested from the cells adhering to each material sample (HAp or α -Al₂O₃ discs),
 7 which reflects the time course of MC3T3-E1 cells on each sample material. Thus, the data
 8 suggests that the cells proliferated on all discs for culture periods up to day 7. However, there
 9 was no significant difference in the cell proliferation between LN-adsorbed discs (samples LN4-
 10 HA, LN8-HA, LN4-AL, and LN8-AL) and untreated discs (samples LN0-HA and LN0-AL) at
 11 each culture period. Moreover, Figure 6 also suggests that the amount of cells that proliferated
 12 on HAp discs on day 7 was significantly higher than on α -Al₂O₃ discs irrespective of the
 13 condition of LN adsorption.



14

1 **Figure 4.** Maximum length of MC3T3-E1 cells adhered to HAp and α -Al₂O₃ discs (mean \pm SD,
2 **P* < 0.05, ***P* < 0.01).



3
4 **Figure 5.** Representative fluorescent microscopic images of MC3T3-E1 cells adhered to HAp
5 and α -Al₂O₃ discs.

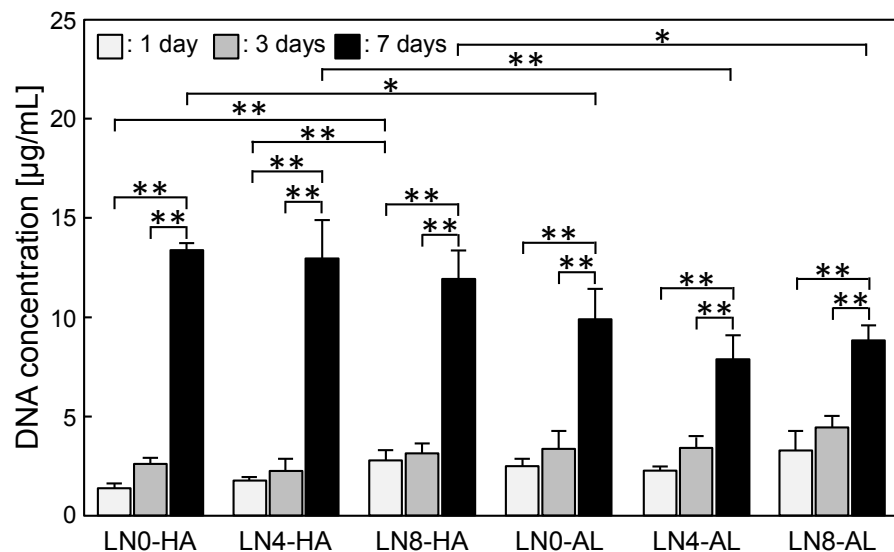


Figure 6. Proliferation of MC3T3-E1 cells on HAp and α -Al₂O₃ discs (mean \pm SD, * P < 0.05, ** P < 0.01).

4. DISCUSSION

4.1. Adsorption of LN on HAp and α -Al₂O₃ powders

The isotherm of LN adsorption on ca-HAp and ca-Al₂O₃ powders in Fig. 1 can be approximated by the Hill equation, which suggests the chemical adsorption of LN on HAp and α -Al₂O₃. In addition, the Hill coefficients larger than 1 for HAp and α -Al₂O₃ imply attractive interactions between LN adsorbed on HAp and α -Al₂O₃²⁷. Based on the previous zeta potential measurements⁸ and the present study (Table 2), both HAp and LN are negatively charged whereas α -Al₂O₃ is positively charged. Therefore, it can be assumed that adsorption of LN on α -Al₂O₃ is attributed to electrostatic attraction. In contrast, adsorption of LN on HAp was expected to be inhibited because of the electrostatic repulsion force between LN and HAp. However, HAp unexpectedly showed a higher adsorption capacity for LN than α -Al₂O₃ (see Fig. 1). These results indicate that there is another interaction mechanism between LN and HAp. It is already

1 known that hydroxyapatite has a hexagonal crystal structure with a positively charged c -face and
2 negatively charged $a(b)$ -face^{30–32}, which raises the possibility that negatively charged LN might
3 specifically adsorb on the positively charged $a(b)$ -face of HAp via isoelectric interaction. We
4 also found that there was no significant difference in the secondary structure of LN adsorbed on
5 samples (Table 3), which supports the idea that a high-ordered structure such as the tertiary
6 structure of LN may largely affect its adsorbing to osteoconductive materials like HAp.

7 The adsorption capacity of LN on $a(b)$ -HAp and c -HAp powders was higher than ca -HAp
8 powder as shown in Fig. 2, but there was no significant difference in the secondary structure of
9 adsorbed LN among HAp powders (Table 3), which implies that the crystal orientation of HAp
10 affects the LN adsorption. LN has some functional domains such as the G domain and domain
11 VI^{13,33}. As shown in Table 4, the isoelectric point of these domains can be estimated *in silico*
12 from the amino acid sequence of LN using the bioinformatics resource portal ExPASy
13 (<http://www.expasy.org/>) operated by the Swiss Institute of Bioinformatics³⁴. These calculated
14 isoelectric points in the functional terminal domains within LN imply that terminal domain IV in
15 the β and γ chains is negatively charged, and terminal domain IV and G domain in the α chain
16 are positively charged in the human body. This variation in charge of the terminal domain of LN
17 may have the potential to control the conformation of adsorbed LN, resulting in specific
18 adsorption of LN on hydroxyapatite although further investigation is needed. In addition, surface
19 properties of the material other than surface roughness, crystal structure, and electrostatic
20 interaction should also be considered in future studies. For instance, the hydrophilicity of a
21 material may affect protein adsorption³⁵.

22 **Table 4.** Calculated isoelectric points of terminal domains of LN.

Terminal domain	Calculated isoelectric point
Terminal domain IV in α chain	9.06
Terminal domain IV in β chain	5.53
Terminal domain IV in γ chain	5.53
G terminal domain in α chain	9.17

4.2. Response of MC3T3-E1 cells to sample attachment

The LN adsorption behavior on HAp and α -Al₂O₃ powder prompted us to investigate MC3T3-E1 cell response to HAp discs with a particular crystal orientation, but it is extremely difficult to obtain HAp discs with a particular crystal plane owing to the extremely small yield of c-HAp powders. Therefore, in the present study, we tried to perform more fundamental investigations to compare the effect of LN adsorption on the attachment of MC3T3-E1 cells to HAp discs that had no particular crystal orientation and α -Al₂O₃ discs. We confirmed that there was no significant difference in surface roughness between the employed sample materials (HAp discs with no particular crystal orientation and α -Al₂O₃ discs) in our previous study⁸. Thus, Fig. 1 shows that the amount of LN adsorbed on HAp (sample LN4-HA) soaked in 0.4 mg/mL LN solution was larger than on α -Al₂O₃ (sample LN4-AL), and that the amount of LN adsorbed on HAp in 0.8 mg/mL LN solution (sample LN8-HA) was similar to that of α -Al₂O₃ (sample LN8-AL). However, it should be noted that the LN concentrations (0.4 and 0.8 mg/mL) used for LN adsorption on discs were much higher than what naturally occurs in human serum (0.81–1.43 μ g/mL)¹⁰ because of the detection limit of our UV-Vis spectrometer and the lower limit of our electronic weighing machine (XPE105, Mettler-Toledo International Inc., USA). Therefore, while the amount of LN adsorbed on the discs in 0.4 and 0.8 mg/mL LN solutions did not necessarily correspond to what would be observed *in vivo*, we were able to perform a fundamental evaluation of the effect of LN adsorbed on HAp and α -Al₂O₃ on attached pre-osteoblastic cells.

1
2
3 1 The number of MC3T3-E1 cells that adhered to samples LN8-HA and LN8-AL was higher
4
5 2 than samples LN0-HA and LN0-AL after the culture period of 6 h and increased during the
6
7 3 observed period up to 6 h, as shown in Fig. 3. These results suggest that the adhesion of MC3T3-
8
9 4 E1 cells onto the untreated HAp and α -Al₂O₃ is poorly initiated during the culture period but is
10
11 5 increased after 6 h of culture when a larger amount of LN has adsorbed onto HAp and α -Al₂O₃,
12
13 6 implying an essential stimulatory effect of adsorbed LN on osteoblast-like cell adhesion²¹.
14
15 7 Serum-containing culture medium, which might interfere with the adsorbed LN, was used for the
16
17 8 MC3T3-E1 cell adhesion assay in this study. However, the LN adsorbed onto HAp and α -Al₂O₃
18
19 9 enhanced MC3T3-E1 cell adhesion as described above, suggesting that the effect of adsorbed LN
20
21 10 on cell adhesion was properly assessed even in the presence of serum-containing cell culture
22
23 11 media. Nevertheless, it is necessary to perform the MC3T3-E1 cell adhesion assay in serum-free
24
25 12 cell culture medium to eliminate interference by serum-derived components.
26
27
28
29
30
31

32 13 Based on the data shown in Figs. 4 and 5, the spreading of MC3T3-E1 cells was significantly
33
34 14 enhanced on LN-adsorbed HAp discs compared with LN-adsorbed α -Al₂O₃ discs treated with
35
36 15 the same LN concentration and culture period. However, there was no significant difference in
37
38 16 the maximum length of MC3T3-E1 cells between sample LN0-HA and sample LN0-AL after the
39
40 17 culture periods of 1 or 6 h. Furthermore, after a culture period of 6 h, although the amount of LN
41
42 18 adsorbed on sample LN8-AL was likely very similar to that on sample LN8-HA, the cell
43
44 19 spreading was significantly enhanced on sample LN8-HA but not on sample LN8-AL. Therefore,
45
46 20 the significant enhancement in the cell spreading on sample LN8-HA could be attributed to the
47
48 21 specific adsorption of LN on HAp but not on α -Al₂O₃, as previously discussed (Figs. 1 and 2 and
49
50 22 Table 3). Consistent with these results, a recent study reported the enhancement of attached
51
52 23 osteoblast-like cells spreading on an LN-coated glass surface²¹. In addition, it was revealed that
53
54
55
56
57
58
59
60

1 the PPFEGCIWN motif, which was identified as a biologically active core-binding sequence
2 within the human laminin $\alpha 2$ chain, promoted cell adhesion and spreading of osteoblast-like
3 cells¹⁸. A similar motif in the α chain of LN adsorbed on sample LN8-HA might contribute to
4 the significant enhancement of osteoblast-like cell adhesion and spreading although the peptide
5 sequence was not identified in this study.

6 Based on the acquired DNA concentrations (Fig. 6), on day 7, the amount of proliferated
7 MC3T3-E1 cells on all of the HAp discs was significantly higher than the α -Al₂O₃ discs,
8 regardless of the LN-adsorption conditions. However, there was no significant difference in the
9 cell proliferation on LN-adsorbed discs and untreated (non-LN-adsorbed) discs. These findings
10 suggest that the proliferation potential of osteoblast-like cells mainly depends on the base
11 material rather than LN adsorbed on the surface. On the other hand, we observed an increase in
12 measured DNA concentration on day 7. These observations could be attributed to a reduced
13 number of cells attached and cultured on the discs. Although we seeded an equivalent amount of
14 MC3T3-E1 cells into each well, there is a possibility that, during the incubation period, some of
15 the seeded cells may have migrated to the narrow portion of the well that was not covered by the
16 discs. In fact, a similar rapid cell proliferation on day 7 was observed when MC3T3-E1 cells
17 were seeded at 625 or 2,500 cells per well directly into the bottoms of wells of non-culture plates
18 with no sample discs. MC3T3-E1 cells proliferated on day 3 when the cells were seeded at
19 10,000 cells per well in the bottoms of wells of non-culture plates with no sample as shown in
20 Fig. 7.

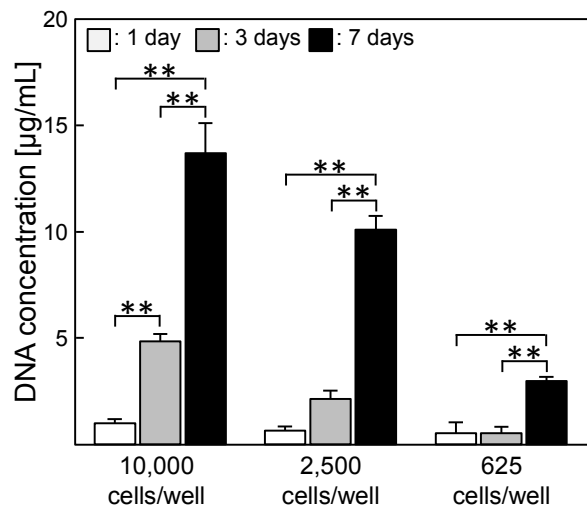


Figure 7. Proliferation of MC3T3-E1 cells seeded at different cell numbers on non-culture wells (mean \pm SD, ** $P < 0.01$).

4. CONCLUSION

We characterized the mode of specific LN adsorption on HAp that remarkably enhances initial attachment and spreading of MC3T3-E1 cells. However, subsequent proliferation of MC3T3-E1 cells mainly depended on the type of material (i.e., HAp or α -Al₂O₃) rather than the mode of LN adsorption onto the materials. These fundamental findings imply that LN adsorbed on HAp could trigger the initial induction of osteoconductivity *in vivo*. Hence, novel biomaterials that specifically adsorb LN could be used to effectively enhance cell attachment and spreading, but further *in vitro* investigations of cell differentiation and *in vivo* experiments are still needed. The present study revealed differences in the effects of LN adsorbed on HAp or α -Al₂O₃ on cell adhesion, spreading, and proliferation but not on differentiation.

AUTHOR INFORMATION

Corresponding Author

1
2
3 1 Masakazu Kawashita, Graduate School of Biomedical Engineering, Tohoku University, TEL:
4
5 2 +81-22-795-3937, FAX: +81-22-795-4735, E-mail: m-kawa@ecei.tohoku.ac.jp
6
7

8 9 3 **Author Contributions**

10
11 4 All authors contributed to writing this manuscript. All authors have approved of the final version
12
13 5 of the manuscript.
14
15

16 17 6 **Funding Sources**

18
19
20 7 This work was partially supported by the Naito Foundation Natural Science Scholarship.
21
22

23 24 8 **ACKNOWLEDGMENTS**

25
26 9 This work was partially supported by the Naito Foundation Natural Science Scholarship. The
27
28 10 authors thank Dr. Tomoyuki Ogawa of Tohoku University for the zeta potential measurements,
29
30 11 Dr. Masanobu Kamitakahara of Tohoku University for the specific surface area measurements,
31
32 12 and Ms. Maiko Furuya of Tohoku University for the cell culture tests.
33
34
35

36 37 13 **ABBREVIATIONS**

38
39 14 HAp, hydroxyapatite; LN, laminin; SSA, specific surface area; FT-IR, Fourier-transform infrared
40
41 15 spectroscopy; PBS, phosphate-buffered saline, UV-Vis, ultraviolet-visible light.
42
43

44 45 16 **REFERENCES**

- 46
47 17 (1) Jarcho, M.; Kay, J. F.; Gumaer, K. I.; Doremus, R. H.; Drobeck, H. P. Tissue Cellular
48
49 18 and Subcellular Events at Bone-Ceramic Hydroxyapatite Interface. *Journal of Bioengineering*
50
51 19 **1977**, *1*, 79-92.
52
53
54
55 20 (2) Aoki, H.; Kato K.; Tabata, T. Osteocompatibility of Apatite Ceramics in Dog's
56
57 21 Mandibles. *Reports of the Institute for Medical and Dental Engineering Japan* **1977**, *11*, 33-35.
58
59
60

- 1
2
3 1 (3) LeGeros, R. Z. Hydroxyapatite. In *An Introduction to Bioceramics*; Hench, L. L.; Wilson,
4 J., Ed. World Scientific: Singapore, 1993, p 139-180.
5
6 2
7
8
9 3 (4) LeGeros, R. Z.; LeGeros, J. P. Hydroxyapatite. In *Bioceramics and Their Clinical*
10 *Applications*; Kokubo, T., Ed.; Woodhead Publishing: Cambridge, 2008, p 367-394.
11
12 4
13
14
15 5 (5) Klein, C. P. A. T.; Wolke, J. G. C.; de Groot, K. Stability of Calcium Phosphate
16
17 6
18
19 7
20
21
22
23 8 (6) Leeuwenburgh, S. G. C.; Wolke J. G. C.; Jansen, J. A. Calcium Phosphate Coatings. In
24
25 9
26
27 10
28
29
30
31 11 (7) Puleo D. A.; Nanci, A. Understanding and Controlling the Bone-Implant Interface.
32
33 12 *Biomaterials* **1999**, *20*, 2311-2321, DOI: 10.1016/S0142-9612(99)00160-X.
34
35
36
37 13 (8) Kawashita, M.; Hayashi, J.; Li, Z.; Miyazaki, T.; Hashimoto, M.; Hihara, H.; Kanetaka,
38
39 14
40
41 15
42
43 16
44
45
46
47 17 (9) Hasegawa, M.; Kudo, T.; Kanetaka, H.; Miyazaki, T.; Hashimoto M.; Kawashita, M.
48
49 18
50
51 19
52
53
54
55
56
57
58
59
60

- 1
2
3
4 1 (10) Kawashita, M.; Hayashi, J.; Kudo, T.; Kanetaka, H.; Li, Z.; Miyazaki, T.; Hashimoto, M.
5
6 2 MC3T3-E1 and RAW264.7 Cell Response to Hydroxyapatite and Alpha-Type Alumina
7
8 3 Adsorbed with Bovine Serum Albumin. *Journal of Biomedical Materials Research Part A* **2014**,
9
10 4 *102*, 1880-1886, DOI: 10.1002/jbm.a.34861.
11
12
13
14 5 (11) Hasegawa, M.; Kudo, T.; Kanetaka, H.; Miyazaki, T.; Hashimoto, M.; Kawashita, M.
15
16 6 Effect of Fibronectin Adsorption on Osteoblastic Cellular Responses to Hydroxyapatite and
17
18 7 Alumina. *Biomedical Materials* submitted.
19
20
21
22 8 (12) Gressner, A. M.; Tittor, W.; Negwer, A.; Pick-Kober, K. H. Serum Concentrations of
23
24 9 Laminin and Aminoterminal Propeptide of Type III Procollagen in Relation to the Portal Venous
25
26 10 Pressure of Fibrotic Liver Diseases. *Clinical Chimica Acta* **1986**, *161*, 249-258, DOI:
27
28 11 10.1016/0009-8981(86)90008-2.
29
30
31
32 12 (13) Aumailley, M.; Bruckner-Tuderman, L.; Carter, W. G.; Deutzmann, R.; Edgar, D.;
33
34 13 Ekblom, P.; Engel, J.; Engvall, E.; Hohenester, E.; Jones, J. C.; Kleinman, H. K.; Marinkovich,
35
36 14 MP.; Martin, G. R.; Mayer, U.; Meneguzzi, G.; Miner, J. H.; Miyazaki, K.; Patarroyo, M.;
37
38 15 Paulsson, M.; Quaranta, V.; Sanes, J. R.; Sasaki, T.; Sekiguchi, K.; Sorokin, L. M.; Talts, J. F.;
39
40 16 Tryggvason, K.; Uitto, J.; Virtanen, I.; von der Mark, K.; Wewer, U. M.; Yamada, Y.;
41
42 17 Yurchenco, P. D. A Simplified Laminin Nomenclature. *Matrix Biology* **2005**, *24*, 326-332, DOI:
43
44 18 10.1016/j.matbio.2005.05.006.
45
46
47
48
49 19 (14) Clark, E. A.; Brugge, J. S. Integrins and Signal Transduction Pathways: the Road Taken.
50
51 20 *Science* **1995**, *268*, 233-239, DOI: 10.1126/science.7716514.
52
53
54
55
56
57
58
59
60

- 1
2
3 1 (15) Yuasa, K.; Fukumoto, S.; Kamasaki, Y.; Yamada, A.; Fukumoto, E.; Kanaoka, K.; Saito,
4
5
6 2 K.; Harada, H.; Arikawa-Hirasawa, E.; Miyagoe-Suzuki, Y.; Takeda, S.; Okamoto, K.; Kato, Y.;
7
8 3 Fujiwara, T. Laminin $\alpha 2$ is Essential for Odontoblast Differentiation Regulating Dentin
9
10 4 Sialoprotein Expression. *The Journal of Biological Chemistry* **2004**, *279*, 10286-10292, DOI:
11
12 5 10.1074/jbc.M310013200.
13
14
15
16 6 (16) Uchida, M.; Oyane, A.; Kim, H. M.; Kokubo, T.; Ito, A. Biomimetic Coating of Laminin-
17
18 7 Apatite Composite on Titanium Metal and Its Excellent Cell-Adhesive Properties. *Advanced*
19
20 8 *Materials* **2004**, *16*, 1071-1074, DOI: 10.1002/adma.200400152.
21
22
23
24 9 (17) Oyane, A.; Uchida, M.; Ito, A. Laminin-Apatite Composite Coating to Enhance Cell
25
26 10 Adhesion to Ethylene-Vinyl Alcohol Copolymer. *Journal of Biomedical Materials Research*
27
28 11 *Part A* **2005**, *72*, 168-174, DOI: 10.1002/jbm.a.30205.
29
30
31
32 12 (18) Yeo, I. S.; Min, S. K.; Ki Kang, H. K.; Kwon, T. K.; Youn Jung, S. Y.; Min, B.M.
33
34 13 Identification of a Bioactive Core Sequence from Human Laminin and its Applicability to Tissue
35
36 14 Engineering. *Biomaterials* **2015**, *73*, 96-109, DOI: 10.1016/j.biomaterials.2015.09.004.
37
38
39
40 15 (19) Yeo, I. S.; Min, S. K.; Ki Kang, H. K.; Kwon, T. K.; Youn Jung, S. Y.; Min, B.M.
41
42 16 Adhesion and Spreading of Osteoblast-like Cells on Surfaces Coated with Laminin-Derived
43
44 17 Bioactive Core Peptides. *Data in Brief* **2015**, *5*, 411-415, DOI: 10.1016/j.dib.2015.09.032.
45
46
47
48 18 (20) Mathews, S.; Bhonde, R.; Gupta, P. K.; Totey, S. Extracellular Matrix Protein Mediated
49
50 19 Regulation of the Osteoblast Differentiation of Bone Marrow Derived Human Mesenchymal
51
52 20 Stem Cells, *Differentiation* **2012**, *84*, 185-192, DOI: 10.1016/j.diff.2012.05.001.
53
54
55
56
57
58
59
60

- 1
2
3
4 1 (21) Schlie-Wolter, S.; Ngezahayo, A.; Chichkov, BN. The Selective Role of ECM
5
6 2 Components on Cell Adhesion, Morphology, Proliferation and Communication In Vitro.
7
8 3 *Experimental Cell Research* **2013**, *319*, 1553-1561, DOI: 10.1016/j.yexcr.2013.03.016.
9
10
11 4 (22) Stea, S.; Savarino, L.; Toni, A.; Sudanese, A.; Giunti, A.; Pizzoferrato, A.
12
13 5 Microradiographic and Histochemical Evaluation of Mineralization Inhibition at the Bone-
14
15 6 Alumina Interface. *Biomaterials* **1992**, *13*, 664-667, DOI: 10.1016/0142-9612(92)90125-8.
16
17
18
19 7 (23) Okada, Y.; Kobayashi, M.; Neo, M.; Shinzato, S.; Matsushita, M.; Kokubo, T.;
20
21 8 Nakamura, T. Ultrastructure of the Interface between Alumina Bead Composite and Bone.
22
23 9 *Journal of Biomedical Materials Research* **2000**, *49*, 106-111, DOI: 10.1002/(SICI)1097-
24
25 10 4636(200001)49:1<106::AID-JBM13>3.0.CO;2-W.
26
27
28
29
30 11 (24) Wang, Y.; Yan, Y.; Dai, H.; Li, M. Preparation of Hydroxyapatite Fibers by the
31
32 12 Homogeneous Precipitation Method. *Journal of Wuhan University Technology Materials Science*
33
34 13 *Edition* **2002**, *17*, 39-41, DOI: 10.1007/BF02838536.
35
36
37
38 14 (25) Zhuang, Z.; Aizawa, M. Protein Adsorption on Single-Crystal Hydroxyapatite Particles
39
40 15 with Preferred Orientation to a(b)- and c-axes. *Journal of Materials Science. Materials in*
41
42 16 *Medicine*. **2013**, *24*, 1211-1216, DOI: 10.1007/s10856-013-4879-4.
43
44
45
46 17 (26) Warburg, O.; Christian, W. Isolation and Crystallization of Enolase. *Biochemische*
47
48 18 *Zeitschrift* **1942**, *310*, 384-421.
49
50
51
52 19 (27) Dolatshahi-Pirouz, D.; Jensen, T.; Foss, M.; Chevallier, J.; Besenbacher, F. Enhanced
53
54 20 Surface Activation of Fibronectin upon Adsorption. *Langmuir* **2009**, *25*, 2971-2978, DOI:
55
56 21 10.1021/la803142u.
57
58
59
60

- 1
2
3 1 (28) Luo, Q. L.; Andrade, J. D. Cooperative Adsorption of Proteins onto Hydroxyapatite.
4
5 2 *Journal of Colloid and Interface Science* **1998**, *200*, 104-113, DOI:10.1006/jcis.1997.5364.
6
7
8
9 3 (29) Shahbeig, H.; Bagheri, N.; Ghorbanian, S. A.; Hallajisani, A.; Poorkarimi, S. A New
10
11 4 Adsorption Isotherm Model of Aqueous Solutions on Granular Activated Carbon. *World Journal*
12
13 *of Modeling and Simulation* **2013**, *9*, 243-254.
14
15
16
17 6 (30) Kawasaki, T.; Niikura, M.; Kobayashi, Y. Fundamental Study of Hydroxyapatite High-
18
19 7 Performance Liquid Chromatography: III. Direct Experimental Confirmation of the Existence of
20
21 8 Two Types of Adsorbing Surface on the Hydroxyapatite Crystal. *Journal of Chromatography*
22
23 **1990**, *515*, 125-148, DOI: 10.1016/S0021-9673(01)89307-9.
24
25
26
27 10 (31) Kawasaki, T. Hydroxyapatite as a Liquid Chromatographic Packing. *Journal of*
28
29 11 *Chromatography* **1991**, *544*, 147-184, DOI: 10.1016/S0021-9673(01)83984-4.
30
31
32
33 12 (32) Kandori, K.; Fudo, A.; Ishikawa, T. Study on the Particle Texture Dependence of Protein
34
35 13 Adsorption by Using Synthetic Micrometer-Sized Calcium Hydroxyapatite Particles. *Colloids*
36
37 *and Surfaces B: Biointerfaces* **2002**, *24*, 145-153, DOI: 10.1016/S0927-7765(01)00227-2.
38
39
40
41 15 (33) Beck, K.; Hunter, I.; Engel, J. Structure and Function of Laminin: Anatomy of a
42
43 16 Multidomain Glycoprotein. *FASEB Journal* **1990**, *4*, 148-160.
44
45
46
47 17 (34) Gasteiger, E.; Gattiker, A.; Hoogland, C.; Ivanyi, I.; Appel, R. D.; Bairoch, A. ExPASy:
48
49 18 The Proteomics Server for in-Depth Protein Knowledge and Analysis. *Nucleic Acids Research*
50
51 **2003**, *31*, 3784-3788, DOI: 10.1093/nar/gkg563.
52
53
54
55
56
57
58
59
60

- 1 (35) Wang, K.; Zhou, C.; Hong, Y.; Xhang, X. A Review of Protein Adsorption on
2 Bioceramics. *Interface Focus* **2012**, 2, 259-277, DOI: 10.1098/rsfs.2012.0012.

3

4

5 TABLE OF CONTENTS GRAPHIC

